The Eurasia Proceedings of Science, Technology, Engineering and Mathematics (EPSTEM)
ISSN: 2602-3199

The Eurasia Proceedings of Science, Technology, Engineering and Mathematics (EPSTEM), 2026

Volume 40, Pages 273-284

ICBAST 2026: International Conference on Basic Sciences and Technology

Analysis of MEMS IMU Errors Impact on UAV Positioning Accuracy

Antofie Bianca-Gabriela
Polytechnic University of Bucharest

Abstract: This paper proposes a comprehensive study conducted over one of the primary sources of positioning errors in unmanned aerial systems (UAVs) navigation systems: the inherent limitations of embedded miniaturized inertial measurement units (IMUs). In recent years, MEMS technologies have come to dominate the electronics market due to their promising advantages of reduced cost and size, low power consumption and series production. These aspects make them particularly attractive for the applications in which compactness and autonomy are critical, such as in the UAV industry. However, the drawbacks of MEMS devices are their susceptibility to environmental factors and their intrinsic imperfection which result in errors and noises contaminating the output acceleration and angular velocity signals. Improper sensing of vehicle dynamics may consequently lead to erroneous computation within the strap-down navigation algorithm. For this reason, errors and noises originating from the inertial subsystem may substantially degrade the precision of the final global coordinates and compromise the overall mission success. The current research aims to provide a clear examination of the aspects influenced by IMU errors throughout the navigation algorithm, as well as to identify potential approaches for further research in the field of positioning accuracy enhancement.

Keywords: UAV navigation systems, Miniaturized inertial measurement units, Strap-down navigation algorithm, IMU errors, Positioning accuracy enhancement

Introduction

In the context of autonomous systems emergence, aerospace manufacturers place significant emphasis on the development of compact avionics, lightweight design, continuous monitoring of operational parameters and successful mission fulfillment. From this perspective, MEMS (Micro-Electro Mechanical Systems) technology has gained popularity in the aerospace sector because it promises to provide key features such as reduced dimension and power consumption, low production costs, while maintaining an optimal performance. (Osiander, 2006)

Unmanned Aerial Vehicles (UAVs) or more familiar drones, represent the future for numerous miliary and civil applications due to the reduced human life risk, full autonomy and enhanced mission flexibility involved. The overall operational behavior of any UAV depends on its capability to maintain stable flight control while executing mission commands either on manual or autopilot mode, functions ensured by its primary component: the navigation system. Modern drones include at least two complementary navigation systems, among which the Global Navigation Satellite System (GNSS), the Inertial Navigation System (INS), radio navigation system and image-based navigation system are the most commonly used (Bekir, 2007; Zhang, 2025).

Satellite navigation represents the main source of navigation data due to its global coverage and long-term accuracy; however, in areas where the signal is jammed or obstructed, at least one secondary system is needed. For instance, the inertial system maintains positioning continuity by virtue of its independence from external factors and superior short-term precision (Grewal, 2020). Radio beacons are also a suitable choice for integration with GPS due to their positioning accuracy on the order of tens of meters. Nevertheless, their performance is highly dependent on the line-of-sight specification of the drone (Arning, 2007). In image-based

- Selection and peer-review under responsibility of the Organizing Committee of the Conference

navigation, the main concept refers to mapping the area surrounding the UAV through image processing techniques and returning its location, relative position and attitude, as well as providing obstacle detection capabilities and visual warnings to the operator (Liao, 2021).

In view of technological advancements over the last decades, nowadays inertial navigation systems come in strap-down architectures in which inertial sensors directly measure the motion of the vehicle to which they are rigidly attached to and combined into an inertial measurement unit (IMU). Moreover, they incorporate a variety of technologies depending on the precision requirements of the application and associated financial constraints; however, MEMS sensors appear to dominate the sensor market compared to other alternative existing solutions.

As a matter of fact, microelectronics rose as a result of the increased interest of researchers in silicon, a material that has proven to possess ideal mechanical and thermal properties for semiconductor fabrication. By means of micromachining techniques, microsystems with sensing or actuation functions have been successfully integrated into micro- and nano-scale chips, thus giving rise to MEMS and NEMS technologies (Choudhary, 2013).

For design reasons, the majority of UAV systems include miniaturized IMUs, typically from mass production provenience. Consequently, the main interest of most producers is on the rapid, large-scale fabrication while preserving the low cost and size, rather than the quality of the product. Factors such as manufacturing imperfections, limitations associated with miniaturization processes and insufficient serial testing significantly affect the precision of these sensors (Liu, 2025).

The sensitive precision of miniaturized IMUs can generate considerable positioning errors and may negatively affect flight control tasks, even if other navigation systems are being used on the respective UAV. Thus, it is essential to understand how these errors influence positioning accuracy, by studying their behavior not only under static conditions, but also in complex dynamic environments (Amirsadri, 2012).

This paper aims to provide an analysis of the main error types specific to MEMS-based IMUs through a two-stage approach. The first part focuses on the identification and characterization of errors by using a simulated sensor model, while the second section evaluates their influence in a real flight scenario, on an integrated INS/GPS navigation system resembling modern architecture.

Overview of MEMS-based Inertial Measurement Units

IMU Architecture Description

An IMU mainly consists of an assembly of inertial sensors - a triad of accelerometers and a triad of gyroscopes - which are incapsulated together in a small chip using micromachining techniques. In inertial navigation systems, IMU provides the measurements of specific forces (which are later corrected with the gravitational acceleration to obtain raw linear accelerations) and angular velocity necessary for further conversion throughout the strap-down navigation algorithm (Titterton, 2005; Grewal, 2020) .

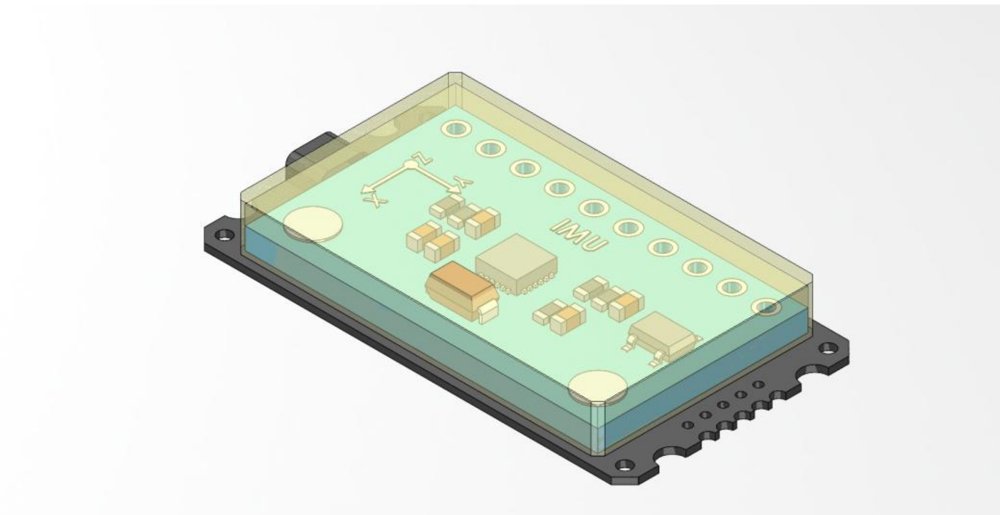

Figure 1. Inertial Measurement Unit packaging

In aerospace applications, these sensors are commonly fabricated in three-axis configurations, maximizing space and simplifying algorithm implementation. Besides accelerometers and gyroscopes, an IMU contains magnetometers, temperature and pressure sensors, a microcontroller, signal processing electronics, a power supply port and output protocols. (TDK Electronics)

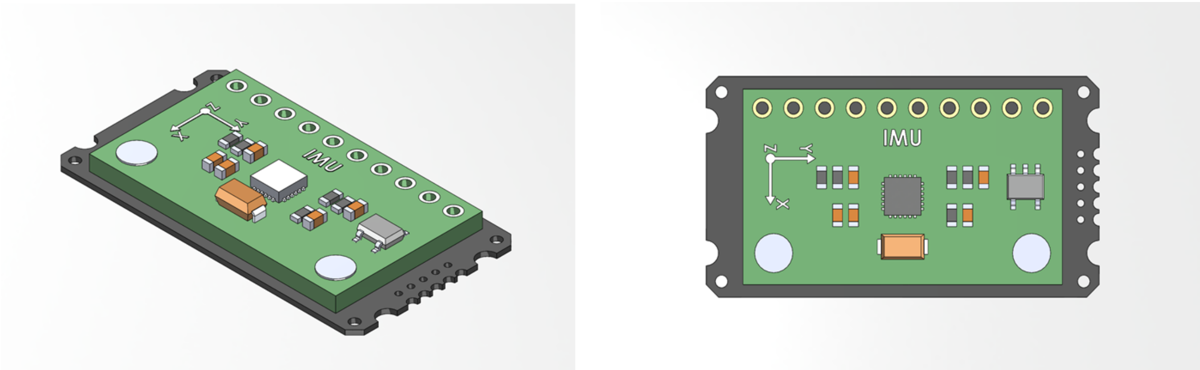

Figure 2. Inertial Measurement Unit PCB layout

The precision class of the IMU defines the scale of the fabrication constraints, therefore, the lower the price, the lower quality of materials, attention to details and time assigned for the respective component. To support sensor performance, there comes interest for research in the areas of error modelling and compensation, signal processing and advanced filtration methods, as well as positioning accuracy enhancement.

Classification of Specific Errors and Noises

MEMS-based inertial sensors generally present two main categories of errors in their output signals, *deterministic* and *stochastic* errors, which tend to accumulate over time if not eliminated and dramatically influence the overall accuracy of the inertial navigator. Both categories of errors are influenced by internal and external factors, including manufacturing imperfections, environmental conditions, mechanical vibrations or shocks and electromagnetic interference. Therefore, an IMU error model should be defined from the earliest stage of system development.

The mathematical equation describing the relation between the input measurements *f(t)* and *ω(t)* and the output signals of the IMU inertial sensors $\tilde{f}(t)$ and $\tilde{\omega}(t)$ can be expressed as (Farrell, 2021):

$$\begin{cases} \tilde{f}(t) = f(t) + d_{acc}(\vec{f}(t)) + s_{acc}(t) \\ \tilde{\omega}(t) = \omega(t) + d_{gyro}(\vec{\omega}(t)) + s_{gyro}(t) \end{cases}, \tag{1}$$

where $d_{acc}(\vec{f}(t)), d_{gyro}(\vec{\omega}(t))$ - deterministic errors of vector measurements $\vec{f}, \vec{\omega}$; s_{acc}, s_{gyro} - stochastic errors.

Deterministic Errors

Deterministic errors, such as biases, scale factors or axis misalignment errors can be determined and eliminated through calibration or compensation algorithms.

In the case of accelerometers, the calibration procedure involves using a mechanical platform for static tests of different positions of the chip, while for gyroscopes, different angle rates are being studied. The sensors are recalibrated when employed on UAVs using similar simple procedures. As a result, IMU sensors datasheet parameters are determined for static states and they may differ considerably in dynamic scenarios depending on the class of precision of the IMU. For tactical IMUs, calibration tests are performed for each unit individually for an appropriate interval of time, while in the commercial category, the emphasis is on high quantity in the shortest amount of time.

Equation (2) illustrates the error model associated to the IMU (Titterton, 2005; El-Diasty, 2008):

$$\begin{cases} \tilde{f} = (1 + SF_f + M_f)\omega + +B_f + \nu_f \\ \tilde{\omega} = (1 + SF_\omega + M_\omega)\omega + G_\omega a + B_\omega + \nu_\omega \end{cases}, \tag{2}$$

where: SF_f, SF_ω - scale factor errors; M_f, M_ω - misalignment matrices; G_ω - g-sensitivity matrix; B_f, B_ω - biases; ν_f, ν_ω - stochastic errors (noises).

Bias is generally defined as the output of the sensor when no force is applied at the input. IMUs present both accelerometer and gyro biases in their static states. Bias error divides itself in turn into a first deterministic part, the systematic offset, and a second random part, the time-varying offset which cannot be predicted over time. Constant bias is experimentally determined in testing phases, with typical accelerometer values starting from 10^{-3}g to even 10^{-6}g, while values for gyroscopes generally range from 10 °/s to 10^{-1} °/s. (Ailneni, 2019)

Scale factor represents the ratio between the output signal and the physical quantity acting along the sensitivity axis of the sensor. The ideal scale factor is 1; however, the error of the calculated value based on the real sensor measurements is different from 1 and this difference is called the scale factor error. General values are placed between 0.01% and 2% for accelerometers and gyroscopes.

Axis misalignment error is a direct consequence of the imperfect component mounting inside the sensor housing. It occurs when the inertial sensors' sensitivity axes are not perfectly orthogonal to one another. Similarly to bias, scale factor and axis misalignment errors can be determined in laboratory tests and are usually eliminated through calibration or compensation algorithms. Their values are situated in the 0.01°-2° interval.

Another deterministic error, specific to gyroscopes, is the *g-sensitivity*, which roots back to their basic functioning principle - mechanical vibration. As a result, linear accelerations may create a false rotational movement and induce erroneous rotational velocity components to the output signal. General values range from 0.1°/h/g to 10°/h/g (Luu, 2007).

Figure 3 depicts the deterministic errors specific to MEMS IMUs.

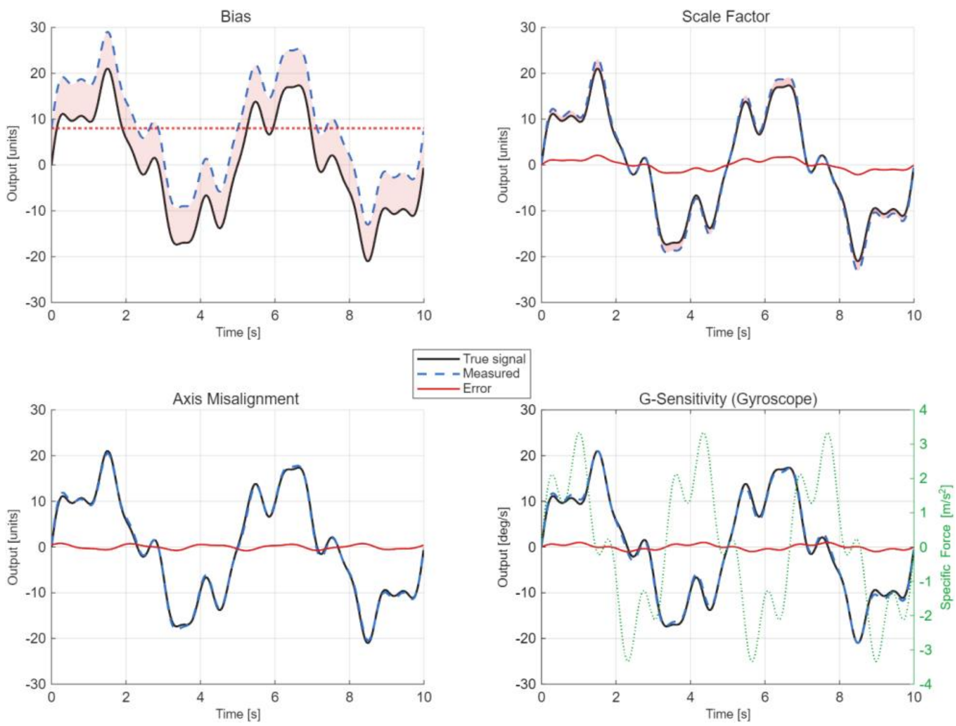

Figure 3. Deterministic errors of MEMS IMUs

Stochastic Errors

In contrast, *stochastic errors* or *noises* represent random processes resulted from unpredictable bias drifts over time or from inherent sensor noise. Unlike deterministic errors, they do not follow a certain path and tend to overlap the good signal, as they vary each time the sensor is powered on. For this reason, these errors must be modelled by identifying the characteristics specific to stochastic processes and correlating them with time over long sampling intervals. The most widely used methods for stochastic error compensation include the Allan variance method, Gauss-Markov models, random state-space error models and other autocorrelation-based techniques (Grigorie, 2010; Farrell, 2022).

Stochastic errors consist of both low-frequency components-such as bias instability and rate random walk-and high frequency components, commonly referred to as noises.

Bias instability, or flicker noise, represents a low-frequency random drift in the sensor output signal and is typically modelled through a random walk or Gauss-Markov model.

Quantization noise is specific to sensors, being produced through analog-to-digital conversion included in the IMU circuitry. It resides in the difference between the amplitude of the sampled points and digital resolution of the ADC (Luu, 2007).

White noise represents the main source of stochastic error in an IMU and it is generally characterized by the noise density parameter. For accelerometers, the corresponding error is the velocity random walk (VRW), whereas for gyroscopes it is defined as angle random walk (ARW). These metrics indicate how measurement noise propagates and accumulates over time, ultimately leading to velocity and orientation accuracy degradation (Hussen, 2015).

Rate random walk (RRW) is derived from white noise and represents the progressive accumulation of noise over time, which results in long-term drift in the measured data.

Figure 4 depicts a graphical representation of the stochastic errors of MEMS-based IMUs.

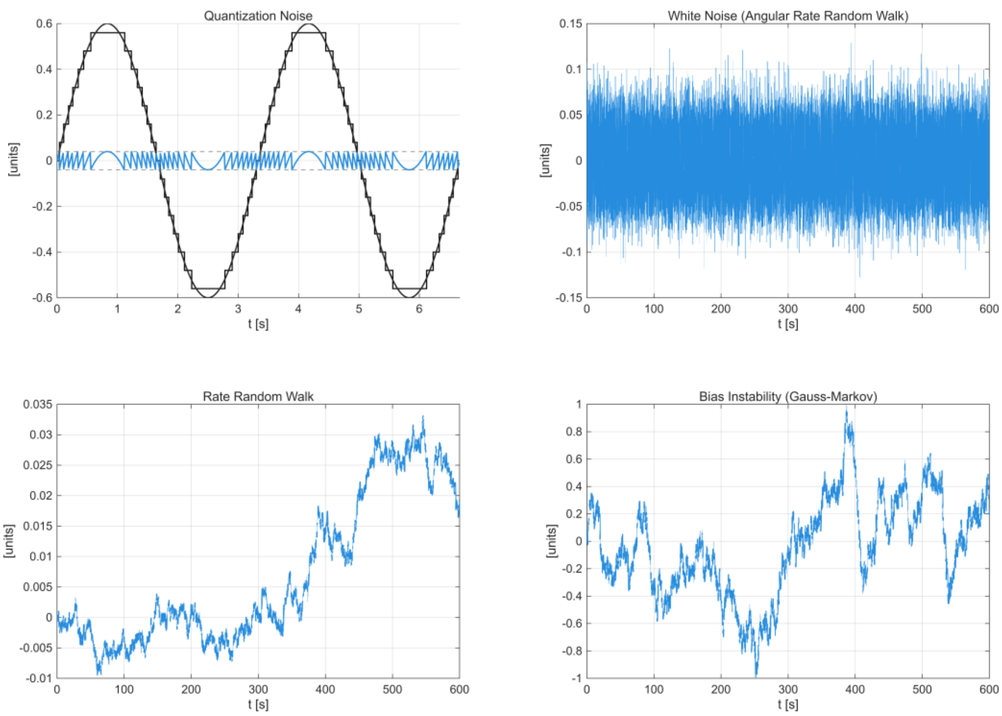

Figure 4. Stochastic errors of MEMS IMUs

Identification and Representation of IMU Errors

For the graphic illustration of the errors previously described, an IMU model developped from IEEE standard models for accelerometers and gyroscopes was implemented in MATLAB/Simulink, as shown in Figure 5. (Grigorie 2005, 2010)

The Analog Devices sensor ADIS16495 was selected for configuring the IMU model. ADIS16495 datasheet error parameters were included in Table 1. (Analog Devices Inc.)

Figure 5. IMU model implemented in MATLAB/Simulink **(Analog Devices Inc.)**

Table 1. ADIS16495 datasheet specifications

Parameter	Gyroscope	Accelerometer
Bias	0.8 °/h	3.2μg
Scale Factor Error	±0.2%	±0.01%
Misalignment Error	±0.05°	±0.035°
G-sensitivity	0.006-0.015°/s	-
ARW/VRW	$0.09\,^{\circ}/\sqrt{h}$	$0.008\ m/s/\sqrt{h}$
Noise density	$0.002\,^{\circ}/\mathrm{sec}/\sqrt{Hz}$	$17\ \mu g/\sqrt{Hz}$

In order to simulate the deterministic errors, a static condition was maintained for a simulation time of 60 seconds, with the following input values: $a_x=a_y=0$ m/s^2, $a_z=-9.80665$ m/s^2, $om_x=om_y=om_z=0$ °/s.

Figure 6 presents the corresponding output signals.

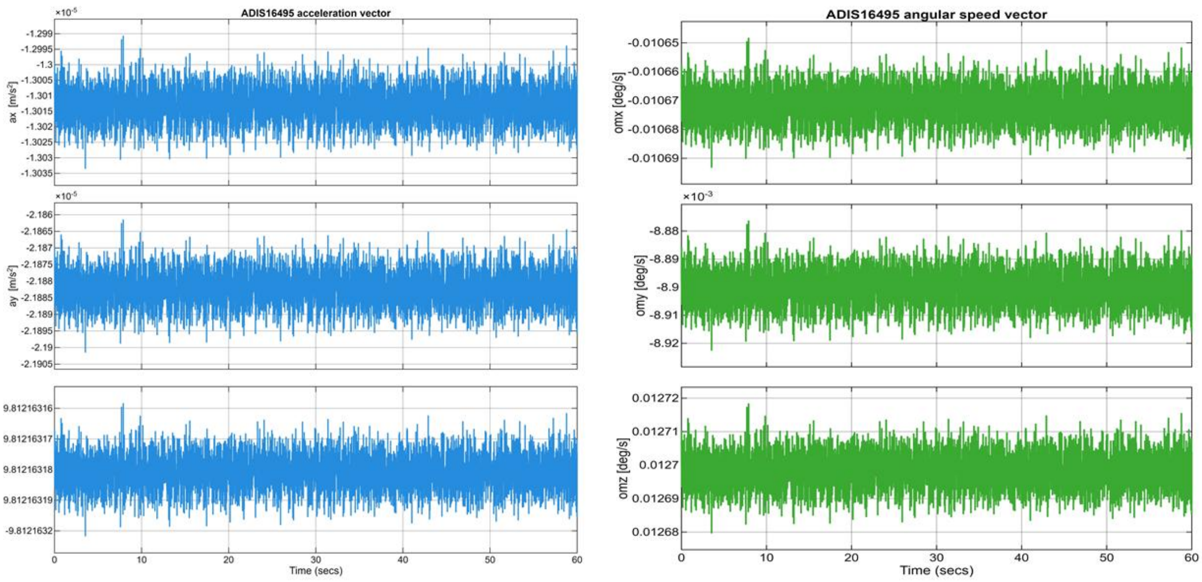

Figure 6. ADIS16495 simulated signals

The mean values of a_x and a_y returned were -1.3013e-05 m/s^2 and -2.1882e-05 m/s^2, respectively. As expected in a static condition, the values are very small and close to zero. According to the sensor datasheet, the expected bias is equal to $3*10^{-4}$, a value that is consistent with the obtained results. The residual low values are produced by the bias and low-frequency stochastic errors.

The mean value of a_z, -9.8122 m/s^2 corresponds to a deviation of -0.0055 m/s² from the input value of gravitational acceleration (9.80665 m/s^2), which suggests the presence of a scale factor error of approximately 0.05% - slightly higher than the ±0.01% specified in the datasheet, but still acceptable for short-term measurements. For the angular speed measurements, the mean values were found to be -0.0107 °/s, -0.0089 °/s, 0.0127 °/s. These results are close to the datasheet value for the gyroscope bias, 0.0002 (0.013 for the simulation time used), confirming the proper implementation of the sensor and the inferior performance of the gyroscope. This demonstrates that the gyroscope model may accumulate a notable amount of bias over longer intervals of time. However, in both cases the signal is visibly perturbed with stochastic errors, which can pose significant challenges for integration whithin the navigation algorithm due to the presence of low and high false frequency components.

For the analysis of stochastic errors, the statistical method of Allan Variance was used. The method works by dividing the signal into time intervals (or clusters) that are multiple of the sample rate and computing the average of the data within each interval (Grigorie, 2010). Allan Variance implies the calculation of differences between consecutive cluster averages and determinating the variance of these differences for each interval length. Then, the log graph of the Allan Variance square root (Allan Deviation) against the cluster time τ gives the characteristic curve that respresents the stochastic errors in the signal (Grigorie, 2012).

In the Allan Deviation plot, each stochastic error follows a particular linear trend, characterized by a specific slope. A slope of -1 corresponds to the quantization noise, a slope of -1/2 indicates white noise, a zero slope is associated with bias instability, while a +1/2 slope characterizes rate or acceleration random walk (Zhao, 2011). For the current case, only the bias instability, white noise and rate random walk have been considered.

Figure 7 depicts the Allan Deviation graph for the IMU simulated signals. As observed, the stochastic trend of the curves can been easily identified from their corresponding slopes.

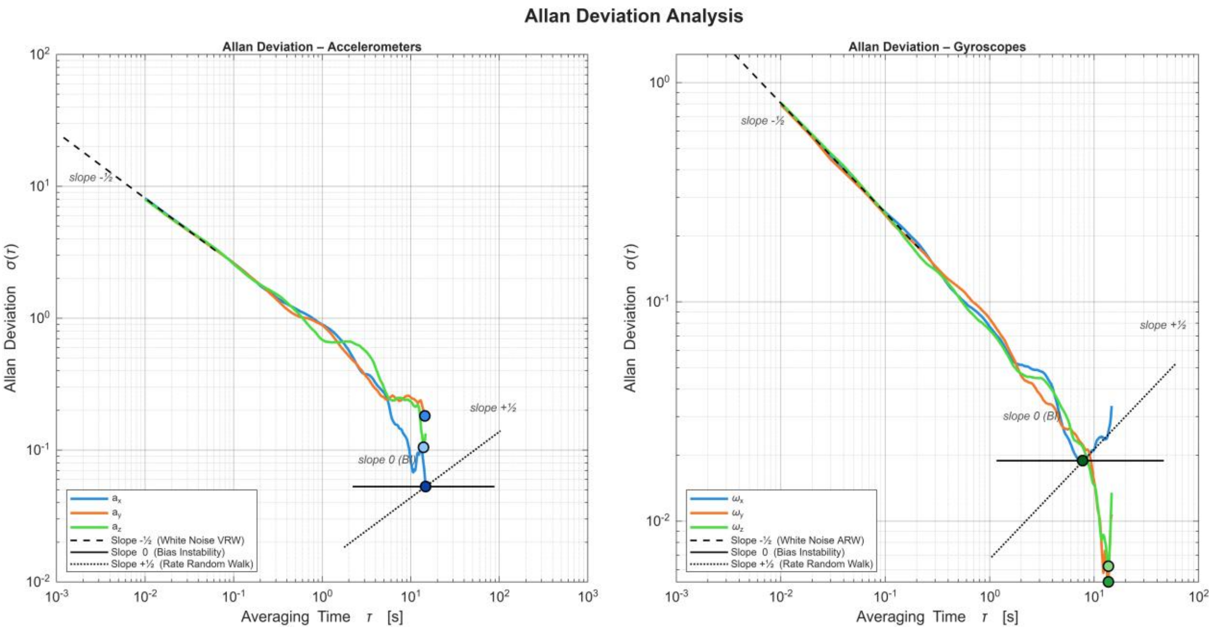

Figure 7. Allan Deviation Analysis of ADIS16495 signals

For the accelerometer, the white noise (VRW) can be identified through the -1/2 slope and is more pronounced at short averaging times (τ<1s). The measured white noise error magnitudes for the acceleration signals are: a_x≈0.8125 m/s^2, a_y≈0.6439 m/s^2, a_z≈0.7946 m/s^2. Bias instability is indicated by the 0 slope, with the corresponding values: a_x≈0.0528 m/s^2, a_y≈0.1815 m/s^2, a_z≈0.1049 m/s^2. Since a_y exhibits the largest bias instability, this may result in more drift on y axis over long-term measurements. The acceleration random walk is visible on slope +1/2 and becomes dominant at large averaging times, with the following values: a_x≈0.0238 m/s^2, a_y≈0.0904 m/s^2, a_z≈0.0491 m/s^2.

Regarding the gyroscopes, white noise is evident at short averaging times (τ<0.1s), with measured values of om_x≈0.0806°/s, om_y≈0.0644°/s, om_z≈0.0726°/s. Bias instability values are: om_x≈0.0189°/s, om_y≈0.0052°/s, om_z≈0.0062°/s, indicating that y and z axes are more stable than the x axis in this sensor model. Finally, rate random walk manifests as an upward slope at high τ, suggesting the accumulation of drift over time. The corresponding values are: om_x≈0.0116°/s, om_y≈0.0048°/s, om_z≈0.0031°/s.

Based on the above results, it can be concluded that among the deterministic errors, bias appears to have the greatest impact on the error propagation into the output signals. Additionally, white noise showed the highest error magnitude, thus also requires more investigation. In the next part of the paper, the influence of bias and white noise errors on the global position provided by the navigation system of an UAV will be examined.

Impact of IMU Errors on Positioning Accuracy

Strap-down Inertial Navigation System Architecture

A strap-down inertial navigation system was implemented in MATLAB/Simulink in accordance with Figure 8 (Grigorie, 2005).

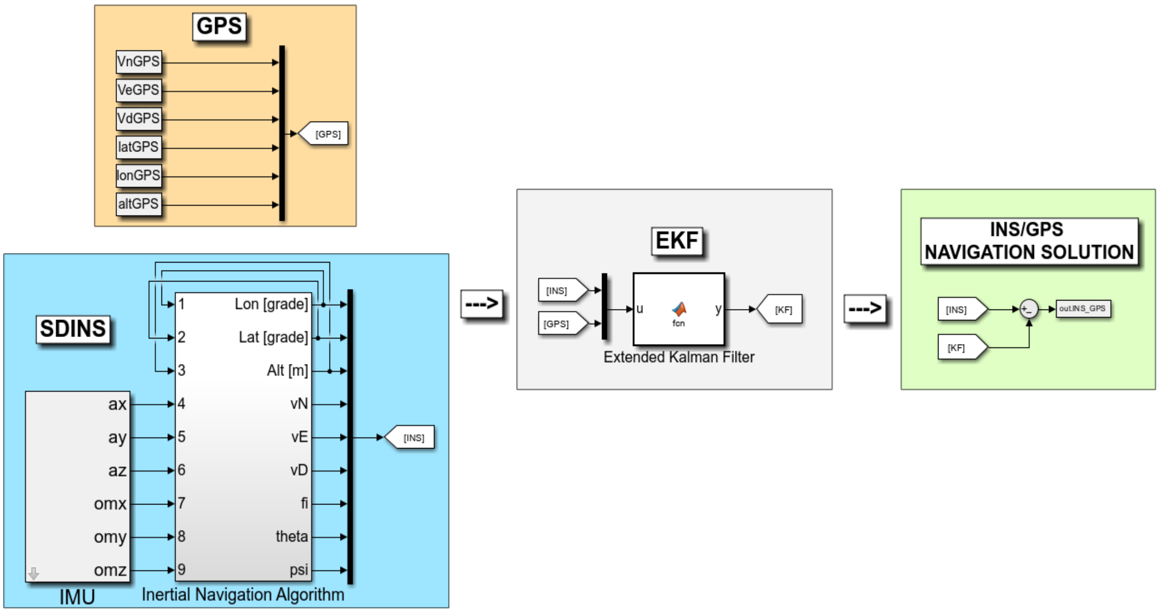

Figure 8. Simulink model of integrated INS/GPS system

The inputs of the navigator are the specific forces and angular velocities measured by IMU. The algorithm comprises two main parts: attitude determination and velocity/position estimation. In the first part, the Euler angles are computed (roll, pitch, yaw), while the second part provides the velocity and position in both North-East-Down (NED) (v_N, v_E, v_D) and Earth-Centered-Earth-Fixed (ECEF) frames, as well as geodetic coordinates (latitude, longitude and altitude) (Titterton, 2005).

In order to reproduce the navigation systems used in modern UAVs, a complementary system was added to the scheme, more exactly the GPS, which provides the speed in the NED frame and the global coordinates. The INS and GPS data are fused using an Extended Kalman Filter in order to correct estimated errors (Jwo, 2013).

Simulation of IMU Errors Effects on Integrated INS/GPS System

For the practical purpose of this study, the INS/GPS integrated architecture was simulated using real-flight data acquisitioned from an IMU mounted on an UAV. The sampling rate of both systems is equal to 100 Hz and the simulation time is set to 250 seconds (4 minutes and 10 seconds). The algorithm was first run with raw signals, and subsequently, errors were amplified in order to observe their impact on the navigation solution.

Firstly, a false bias value was introduced to IMU signals, as follows: 0.05 m/s^2 for accelerometers and 0.001 °/s for gyroscopes. This proved to have a direct influence on all three geodetic coordinates, but especially on the altitude, which dramatically decreased, simulating an accelerated descent scenario. Figure 9 shows the before and after estimated error given by the EKF.

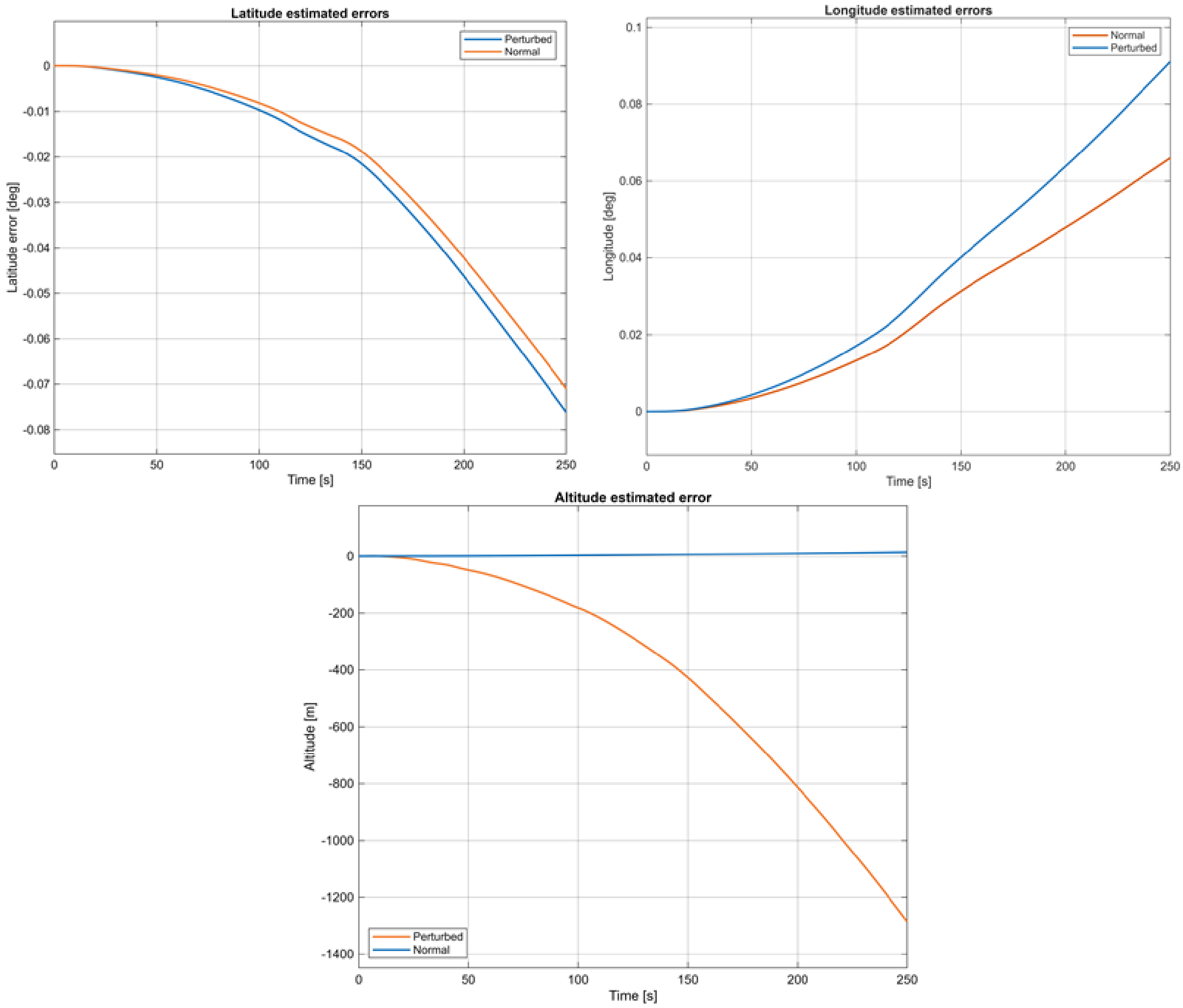

Figure 9. Estimated error results for normal and perturbed inputs (1)

For the latitudinal component, the statistical parameters obtained for the normal inputs were: m=-0.021, σ=0.021 and RMS=0.0296. After the introduction of artificial bias, the parameters became: mean=-0.023, σ=0.023 and RMS=0.0324. In this context, mean and RMS are particularly relevant, as they provide the signal's offset and dispersion around its mean. The perturbation of the input signals produced an increase of approximately 9.5% for each parameter over just four minutes of simulation. Although the EKF effectively manages the bias introduction, larger deviations may accumulate over longer time intervals.

The longitude estimated errors produced the following statistical parameters: m=0.0254, σ=0.020 and RMS=0.0329 in the initial case, and m=0.0336, σ=0.029 and RMS=0.044 in the second case. The raise was more notable in this case, being equal to approximately 33% for the mean and RMS, and 45% for the standard deviation. The longitude drift is highly influenced by the flight direction of the UAV and more pronounced in this case, due to the accumulation of gyro biases in the north and down directions (Cai, 2016).

Lastly, for the altitude component, the initial simulation provided the following values: m=5.597, σ=4.453 and RMS=7.153, with a maximum estimated altitude error of 15.195m. In the second simulation, the results were: m=-414.169, σ=384.793 and RMS=565.328, with a minimum value of -1285.84, thus simulating a sudden drop the UAV according to the INS data. The larger altitude error is given by the inherent sensitivity of the altitude component to biases, specifically the errors induced in the z-axis specific force, which accumulate by consecutive integration. (Li, 2025) The artificial 0.05 m/s^2 acceleration bias introduced to the accelerometers generates a theoretical altitude drift of approximately 1440m for the current flight time. This is consistent with the 1285.84 m value obtained in the simulation.

In the stochastic errors part, white noise was added to the input signals, starting from the following general values for the Noise Density: $0.17\, mg/\sqrt{Hz}$ for the accelerometers and $0.03\,^{\circ}/\sec/\sqrt{Hz}$ for the gyroscopes.

The Noise Power was calculated in accordance with these values. The estimated errors before and after the perturbation of the signals are depicted in Figure 10.

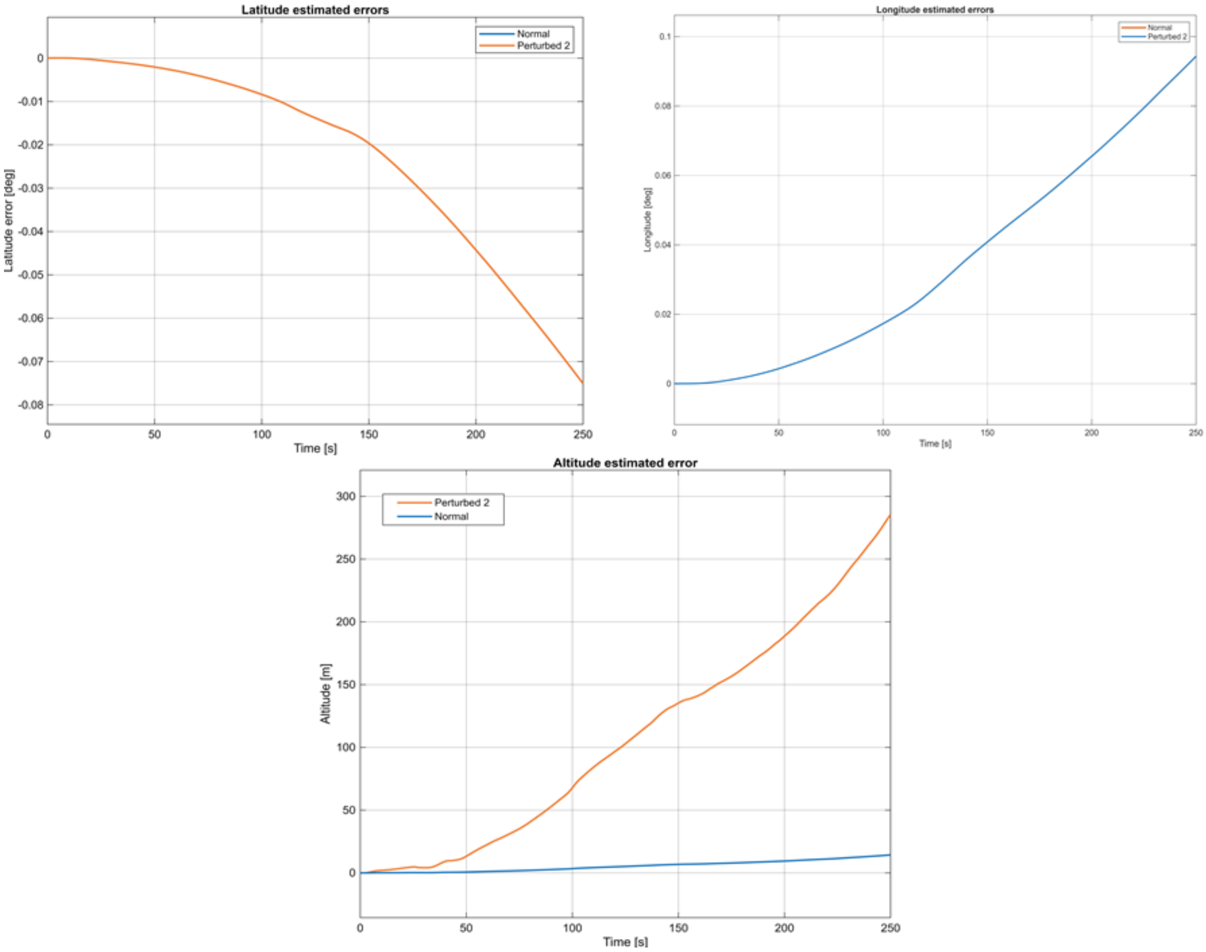

Figure 10. Estimated error results for normal and perturbed inputs (2)

In the second part of the experimental test, the introduction of a white-noise component into the input measurements caused minor deviations in longitude and latitude of 10^{-3} order. Nonetheless, the altitude component was clearly affected. The statistical parameters obtained were: m=107.3620, σ=84.122 and RMS=136.392, with a maximum error of 285.490 m, simulating a false altitude climb of the UAV. Once again, the altitude is influenced by the time integration of z-axis noise. Based on the magnitude of the white-noise introduced to the accelerometers, a theoretical altitude error of approximately 200 m was expected, which aligns consistently with the RMS and maximum values observed in this simulation.

Results and Future Prospects

In the first experimental part of this paper, both deterministic and stochastic errors of an IMU were studied under static conditions in a MATLAB/Simulink model. Among the deterministic errors, bias and scale factor error were found to have the greatest impact. In the case of stochastic errors, white noise and bias instability were identified as the most dominant sources. Consequently, bias and white noise were selected for further analysis in the second phase of the research.

The second experimental test focused on analyzing the impact of IMU errors on the navigation solution of an integrated navigation system similar to those used on modern UAVs. To this end, bias and white noise were artificially introduced into the IMU measurements. The study of bias effects showed that latitude and longitude experienced minor changes on the order of 10^{-2}, which may accumulate over longer time periods, with only longitude showing larger deviations. Altitude was, however, the most influenced by bias, with errors of up to 1300 m. When the white noise was introduced, latitude and longitude did not change significantly, with errors on the order of 10^{-3}, while the altitude error estimate reached almost 285 m.

Future prospects based on the current results include laboratory testing of industrial and tactical IMU sensors, as well as investigating the influence of external factors on the error propagation. Moreover, another field worth of further research refers to a broader range of evaluated errors, assessing the impact of the remaining deterministic and stochastic errors on positioning accuracy, and studying the combined effects of these errors.

Conclusion

This study was conducted under the premise that errors specific to miniaturized IMUs significantly disturb inertial navigation system outputs and the total accuracy of the navigation system. The problem was examined from two perspectives. In the first, low-level analysis was performed, deterministic and stochastic errors were closely evaluated to quantify the impact of each. Secondly, the problem was investigated from high-level perspective, the focus was placed on a navigation system resembling those included into modern UAVs. The influence of the most significant IMU errors was evaluated by artificially amplifying their magnitude and comparing the resulting geodetic parameters with the true values. The results demonstrate the negative impact that inherent IMU errors can have on the positioning accuracy of the monitored vehicle over short intervals of time. For longer flight durations and more complex scenarios, these effects would definitely be more pronounced and result in higher error levels.

In the light of the aforementioned aspects, the propagation of IMU errors throughout the inertial navigation algorithm, and their subsequent fusion with other navigation systems, can substantially impact UAV trajectory and autopilot performance, particularly over extended line-of-sight distances or in signal spoofing or blockage conditions, thereby jeopardizing the overall mission success.

Scientific Ethics Declaration

* The authors declare that the scientific ethical and legal responsibility of this article published in EPSTEM journal belongs to the authors.

Conflict of Interest

* The authors declare that they have no conflicts of interest.

Funding

* This research received no specific grant from any funding agency in the public, commercial, or not-for-profit sectors.

Acknowledgements or Notes

* This article was presented as an oral presentation at the International Conference on Basic Sciences and Technology (www.icbast.net) held in Konya/Türkiye on April 02-05, 2026.

References

Analog Devices Inc. (n.d.). *ADIS16495 data sheet*. Retrieved from https://www.analog.com/media/en/technical-documentation/data-sheets/adis16495.pdf

Ailneni, S. K. (2019). Characterization of MEMS based inertial measurement unit. *IEEE Xplore*. Retrieved from https://ieeexplore.ieee.org

Amirsadri, A. K. (2012). Practical considerations in precise calibration of a low-cost MEMS IMU for road-mapping applications. *IEEE.* Retrieved from https://ieeexplore.ieee.org

Arning, R. K. (2007). *UAV/UCAV navigation systems – Present and potential future*. EADS Innovation Works. München, Germany. Retrieved from https://www.fzt.haw-hamburg.de/pers/Scholz/ewade/2007/

Bekir, E. (2007). *Introduction to modern navigation systems*. World Scientific Publishing Co.

Cai, Q. Y. (2016). Analysis and calibration of the gyro bias caused by geomagnetic field in a dual-axis rotational inertial navigation system. *Measurement Science and Technology, 27(10),* 105001

Choudhary, V. I. (2013). *MEMS: Fundamental technology and applications* (1st ed.). CRC Press.

El-Diasty, M. (2008). Calibration and stochastic modelling of inertial navigation sensor errors. *Journal of Global Positioning Systems, 7(2),* 170-182.

Farrell, J. A. (2021). *IMU error modeling tutorial: INS state estimation with real-time sensor calibration*. eScholarship, California Digital Library. Retrieved from https://escholarship.org

Farrell, J. A. (2022). Inertial measurement unit error modeling tutorial: Inertial navigation system state estimation with real-time sensor calibration. *IEEE Control Systems*.

Grewal, M. S. (2020). *Global navigation satellite systems, inertial navigation, and integration*. Wiley.

Grigorie, T. L. (2005). *Traductoare accelerometrice și girometrice*. Craiova: Sitech.

Grigorie, T. L. (2010a). Analysis of the miniaturized inertial sensors stochastic errors with the Allan variance method: A review. In *Proceedings of the International Conference of Aerospace Sciences "AEROSPATIAL 2010"* (pp. 428–437). Bucharest.

Grigorie, T. L. (2010b). Concepts for error modeling of miniature accelerometers used in inertial navigation systems. *Annals of the University of Craiova, Electrical Engineering Series*.

Grigorie, T. L. (2012). Allan variance analysis of the miniaturized sensors in a strap-down inertial measurement unit. In *International Multidisciplinary Scientific GeoConference* (pp. 443–450).

Grigorie, T. L. (2016). MEMS INS/GPS integrated structure evaluation with experimental data. *IEEE*. Retrieved from https://ieeexplore.ieee.org

Hussen, A. A. (2015). *Low-cost inertial sensors modeling using Allan variance. Zenodo*. Retrieved from https://zenodo.org

Jwo, D. C. (2013). GPS/INS integration accuracy enhancement using the interacting multiple model nonlinear filters. *Journal of applied research and technology, 11(4),* 496-509.

Li, W. W. (2025). Calibration and compensation of gyro drift errors based on external rotational angle comparison in a rotational inertial navigation system. *Applied Sciences*, *15*(3), 1667.

Liao, J. L. (2021). Enhancing navigation performance through visual-inertial odometry in GNSS-degraded environment. *GPS Solutions*. Retrieved from https://link.springer.com

Liu, Z. Y. (2025). Research progress in the relationship between packaging structures and service performance of MEMS inertial sensors. *Frontiers in Materials*. *12*, 1655566.

Luu, H. T.-T. (2007). Errors determination of the MEMS IMU. *VNU Journal of Science*. Retrieved from https://vjs.ac.vn

Osiander, R. A. (2006). *MEMS and microstructures in aerospace applications*. CRC Press.

TDK Electronics. (n.d.). *MPU-9255 data sheet*. Retrieved from https://www.alldatasheet.com/html-pdf/1140875/TDK/MPU-9255/343/5/MPU-9255.html

Titterton, D. W. (2005). Strapdown inertial navigation technology (2nd ed.). *IEEE Aerospace and Electronic Systems Magazine*.

Zhang, Y. L. (2025). *UAV and sensors applications for navigation and positioning*. MDPI Books. Retrieved from https://www.mdpi.com

Zhao, Y. H. (2011). Stochastic modelling and analysis of IMU sensor errors. Archives of Photogrammetry, Cartography and Remote Sensing. Retrieved from https://apcrs.pl

Author(s) Information

Antofie Bianca-Gabriela
Polytechnic University of Bucharest
Doctoral School of the Faculty of Aerospace Engineering
Splaiul Independentei no. 313, sector 6, Bucharest, Romania
ORCID iD: https://orcid.org/0009-0002-8925-6362
*Contact e-mail: *bianca.antofie1512@stud.aero.upb.ro*

To cite this article:

Bianca-Gabriela, A. (2026). Analysis of MEMS IMU errors impact on UAV positioning accuracy. *The Eurasia Proceedings of Science, Technology, Engineering and Mathematics (EPSTEM), 40,* 273-284.